JOC The Journal of Organic Chemistry

pubs.acs.org/joc Article

Mechanisms of Orthogonal Photodecarbonylation Reactions of 3-Hydroxyflavone-Based Acid–Base Forms

Marina Russo, Peter Štacko, Dana Nachtigallová, and Petr Klán*

Cite This: https://dx.doi.org/10.1021/acs.joc.9b03248 Read Online

ACCESS | Metrics & More | Article Recommendations | Supporting Information

ABSTRACT: Carbon monoxide is a naturally occurring gasotransmitter combining inherent toxicity with a remarkable therapeutic potential and arduous administration. Photoactivatable carbon monoxide-releasing molecules (photoCORMs) are chemical agents that allow for precise spatial and temporal control over the CO release. In this work, we present a comprehensive mechanistic study of the photochemical CO release from 3-hydroxy-2-phenyl-4*H*-chromen-4-one, a π-extended 3-hydroxyflavone photoCORM, in methanol using steady-state and transient absorption spectroscopies and quantum chemical calculations. The multiplicity of the productive excited states and the role of oxygen (O_2) in the CO production are emphasized, revealing a photoreaction dichotomy of the 3-hydroxyflavone acid and base forms. The utilization of three major orthogonal mechanistic pathways, all of which lead to the CO release, can fuel future endeavors to improve the CO release efficacy of 3-hydroxyflavone-based derivatives and refine their potential medical applications as photoCORMs.

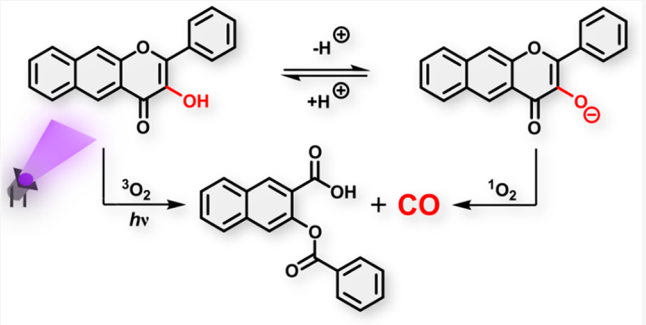

INTRODUCTION

Carbon monoxide (CO) is a small gaseous molecule known for its toxicity, which stems from its higher affinity for hemoglobin than oxygen resulting in the formation of carbonylhemoglobin (COHb) and subsequent hypoxia.[1] On the other hand, CO is a naturally occurring cell-signaling molecule that exhibits strong cytoprotective,[2] cardioprotective,[3] anti-inflammatory,[4] and anti-microbial effects[5] at submicromolar concentrations (0.2 μM).[6] CO was also shown to induce an anti-Warburg effect.[7] Cancer cells and tumors exposed to CO are compelled to rapidly fuel oxidative metabolism, imposing extreme oxidative stress on cells, leading to growth inhibition, cellular exhaustion, and eventually death.[8] The synergistic effect between CO and chemotherapeutics is especially attractive as demonstrated by an increased sensitivity of cancer cells toward camptothecin and doxorubicin upon exposure to CO, while simultaneously protecting normal cell growth and viability.[8]

Despite its remarkable therapeutic potential, one of the central challenges associated with CO therapy is controlling its local biological concentrations. This necessity has spurred the development of CO-releasing molecules (CORMs). Enzymatically triggered processes[9] or a solvent-mediated ligand exchange[6] usually result in a poor spatial and temporal control over the release profile. On the contrary, prevalent CO-releasing metal–carbonyl complexes[10−12] retain a metal backbone upon CO release, which can lead to unwanted reactions with adjacent cells.[13]

Recently, transition-metal-free light-activated CORMs (photoCORMs) have emerged with the promise of circumventing these challenges. A number of organic molecules, such as cyclopropenones,[14] 1,3-cyclobutadiones,[15] or 1,2-dioxolane-3,4-diones,[16] liberate CO upon irradiation with biologically adverse UV light. Cyclic aromatic α-diketone-[17] and xanthene-based carboxylic acids[18,19] were shown to undergo CO liberation initiated with visible light. A *meso*-carboxy BODIPY reported by our group recently is currently the only transition-metal-free photoCORM operating at the edge of a photo-therapeutic window.[20]

Berreau and co-workers have introduced a new type of photoCORM, 3-hydroxy-2-phenyl-4*H*-chromen-4-one (**1**, Figure 1), based on a 3-hydroxyflavone (flavonol) motif, which efficiently releases CO upon irradiation with visible light (λ_{max}^{abs} > 400 nm) under biologically compatible conditions.[21] This structure belongs to the family of flavonoids that are well-known natural antioxidants due to their ability to react with different reactive oxygen species.[22−24] 3-Hydroxyflavone derivatives were reported to undergo an oxygen-mediated enzymatic[25] reaction to release CO in bacteria and fungi. CO can also be produced from these compounds upon irradiation with UV light.[26,27]

3-Hydroxyflavone as an archetypal molecule exists in both acid (**2A**) and base (**2B**) forms (Figure 1), and their

Received: December 2, 2019

https://dx.doi.org/10.1021/acs.joc.9b03248
J. Org. Chem. XXXX, XXX, XXX−XXX

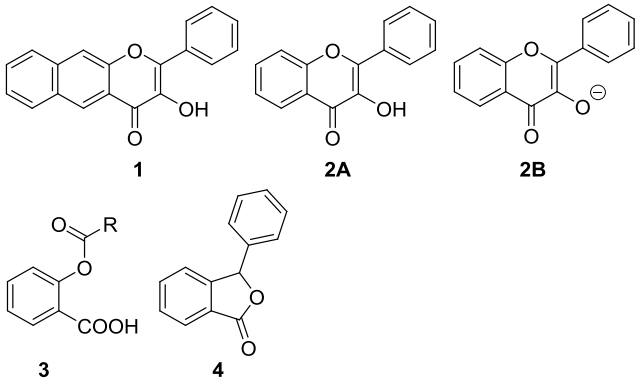

Figure 1. 3-Hydroxyflavone derivatives and the photoproducts obtained by irradiation of **2**.

photophysics and photochemistry have already been investigated in detail. The singlet excited state ^{1}**2A*** undergoes rapid (<125 fs) excited-state intramolecular proton transfer (ESIPT) resulting in the formation of a Stokes-shifted emitting phototautomer (zwitterion) ^{1}**2Z*** (Scheme 1).[28−31] Mat-

Scheme 1. Excited-State Intramolecular Proton Transfer upon Irradiation of 2A

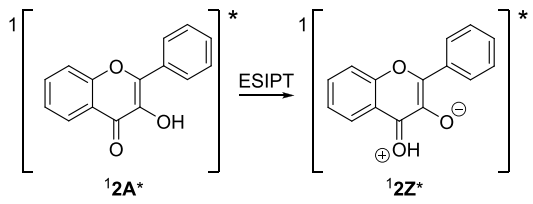

suura[32−34] and later Chou[35,36] and their co-workers have studied the mechanism of CO photoproduction in the presence and absence of molecular oxygen. Several different reaction pathways in solvents of different polarity have been proposed to show that ground-state oxygen, as well as excited (singlet) oxygen, can act as an oxidant in the production of salicylic acid ester **3** and CO, whereas a lactone (**4**) along with CO is formed under anaerobic conditions (Figure 1).

The π-extended 3-hydroxyflavone derivative **1** and its derivatives, proposed and studied by Berreau and co-workers, represent photoCORMs absorbing at longer wavelengths than **2** and releasing CO in high chemical and quantum yields.[20,21,31,37−39] In addition, incorporating logic gate features such as thiol sensing and anti-cancer/anti-inflammatory effects of CO photoreleased from this scaffold has been demonstrated.[31,37] The effects of solvent polarity or the presence of oxygen, metal ions, and proteins[20] has been studied to rationalize the biological applications of **1** as a photoCORM. The mechanism of CO liberation from **1** was assumed to be similar to that of **2**, but it has not been studied in detail yet.

In this paper, we report a kinetic study of the photochemistry of both the acid and base forms of **1** in methanol using steady-state, femtosecond pump−probe and nanosecond laser flash spectroscopies and quantum chemical calculations. We present a comprehensive mechanistic scheme to reveal the multiplicity of the productive excited states and to emphasize and specify the role of oxygen (O_2) in the CO production.

RESULTS AND DISCUSSION

Steady-State Spectroscopy. 3-Hydroxy-2-phenyl-benzo-[*g*]chromen-4-one **1** exists as an acid (**1A**) form or a base (**1B**) form (Scheme 2) in protic solvents.[40] The phenolic hydrogen

Scheme 2. Acid−Base Equilibrium of 1: Formation of Excited Tautomer ^{1}1Z*

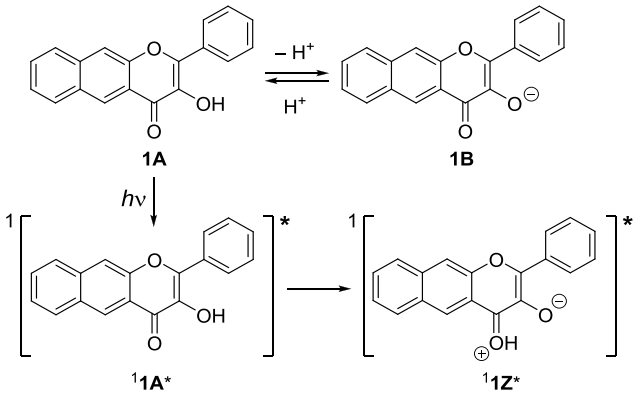

acidity of **2A** in the electronic ground state in an ethanol/water (1:1) solution was determined to be pK_a = 9.60 (and pK_a = 9.81, when extrapolated to pure water) by Rodembusch and co-workers.[41] In this work, we found the pK_a of **1** in a water/DMSO (1:1) mixture to be 9.25 ± 0.03 (the value is corrected for this solvent mixture;[42] Figure 1a). The absorption spectrum of **1A** in this solvent shows two major bands at λ_{max}^{abs} = 344 and 401 nm (Figure 2a, black line), whereas that of **1B** exhibits a single band with λ_{max}^{abs} = 472 nm (Figure 2a, red line). Owing to the poor solubility of flavonol **1** in aqueous media and especially the need to use highly concentrated samples for transient spectroscopy measurements, further experiments were carried out in methanol as a solvent. The conjugate acid **1A** is the sole species observed in a methanol solution. Figure S7 depicts the transition of **1A** to **1B** upon the addition of methanolic sodium methoxide, the spectra of which are essentially identical (**1A**, λ_{max}^{abs} = 345 and 399 nm; **1B**, λ_{max}^{abs} = 474 nm; Figure 2b) to those observed in water/DMSO.

The emission spectrum of the conjugate acid **1A** in methanol exhibits two distinct bands: a very weak fluorescence band at λ_{max}^{em} = 472 nm and an intense band at λ_{max}^{em} = 595 nm (Table 1; Figure 2b). The former signal corresponds to the "normal" excited-state ^{1}**1A***, whereas the latter one is assigned as a phototautomer (zwitterion) ^{1}**1Z*** on the basis of spectroscopic studies with parent flavonol **2A** (Scheme 1). A Stokes shift of over 200 nm (Figure 2b) for this species is the result of an efficient excited-state intramolecular proton transfer (ESIPT), identified and studied for 3-hydroxyflavone **2A**[28,30,43] and also for its π-extended analogue **1**.[20] The fluorescence quantum yields were determined for each emission band to show that the emission from the phototautomer is approximately 30 times more intense than that from ^{1}**1A***. The emission spectrum of **1B** displays only a single, less intense emission band,[44,45] with λ_{max}^{em} at 637 nm (Table 1, Figure 2b).

Photochemistry. The photochemistry of both **1A** and **1B** (1.5 equiv of $NaOCH_3$) in methanol solutions (irradiated at λ_{irr} = 405 and 450 nm, respectively) was investigated, and the course of the reaction was monitored using UV−vis absorption spectroscopy (Figure 3). The disappearance quantum yield of

https://dx.doi.org/10.1021/acs.joc.9b03248
J. Org. Chem. XXXX, XXX, XXX−XXX

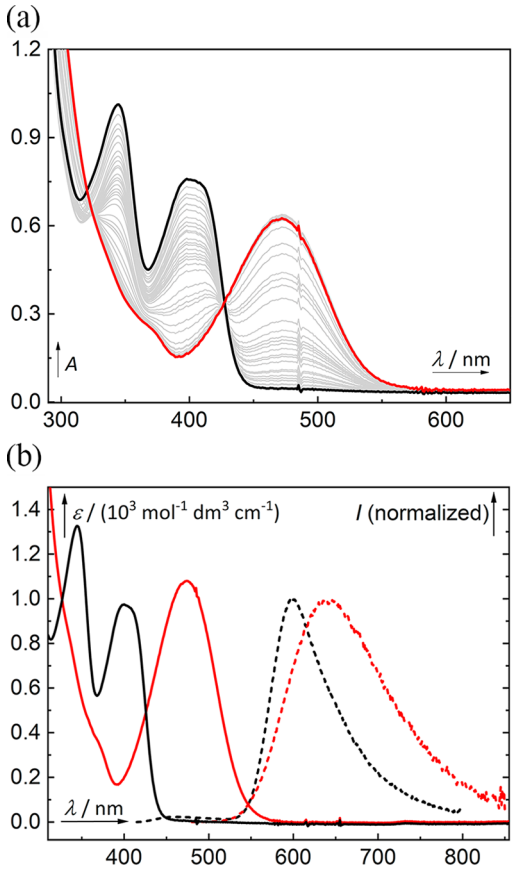

Figure 2. (a) Spectroscopic determination of the pK_a of **1** in water/DMSO (1:1), depicting two distinct absorption bands of **1A** (pH = 6.1, black bold line) and **1B** (pH = 12.3, red bold line) with an isosbestic point at 427 nm. Volume changes in the titration were corrected. (b) Absorption (solid lines; left ordinate) and normalized emission (dashed lines; right ordinate) spectra of **1A** (black; in neat solvent) and **1B** (red; with 1.5 equiv of $NaOCH_3$) in methanol.

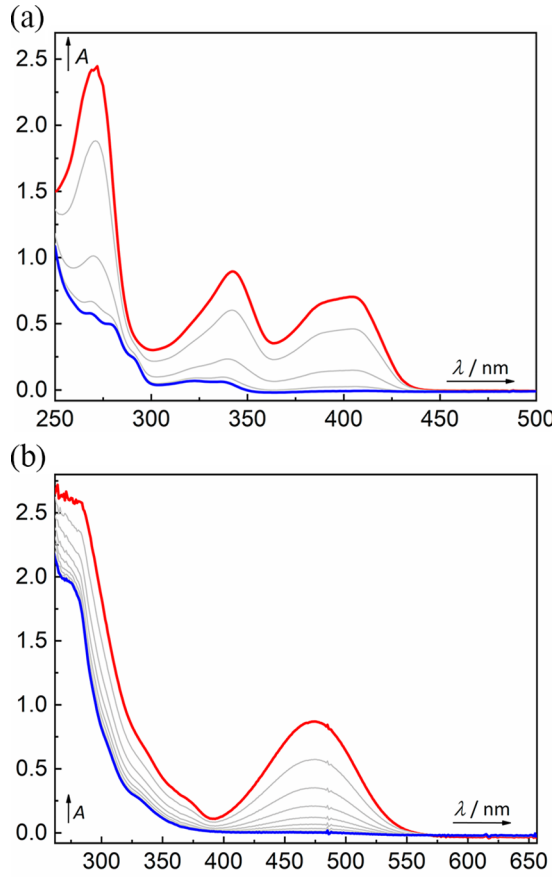

Figure 3. Irradiation of (a) **1A** at λ_{irr} = 405 nm (the absorption spectra were taken every 5 s) and (b) **1B** at λ_{irr} = 450 nm (the absorption spectra were taken every 30 s) in aerated methanol. The spectra prior to (red line) and after (blue line) irradiation are highlighted.

1A in an aerated solution was found to be $\Phi_r = (3.1 \pm 0.1) \times 10^{-2}$ (Table 2). It compares well to that reported for the photochemistry of **1A** in an acetonitrile solution, $\Phi_r = (0.7 \pm 0.02) \times 10^{-2}$.[38] Practically no absorption above 300 nm remained after exhaustive photolysis. The photolysis of **1A** in a methanol solution degassed by three freeze−pump−thaw cycles was more than 2 orders of magnitude less efficient ($\Phi_r \sim 1.2 \times 10^{-4}$), demonstrating a profound influence of oxygen on the reaction course (Figure S12). In addition, the photodegradation of **1B** (1.5 equiv of $NaOCH_3$) in aerated methanol at λ_{irr} = 450 nm was nearly 3 orders of magnitude more efficient ($\Phi_r = (2.1 \pm 0.1) \times 10^{-2}$) than that in a solution degassed by three freeze−pump−thaw cycles ($\Phi_r \sim 1.0 \times 10^{-5}$; Table 2).

The samples of **1** in methanol solutions were irradiated to complete conversion and were analyzed by HPLC and GC-headspace to monitor the photoproducts: 3-(benzyloxy)-2-naphthoic acid **5**, 3-phenylnaphtho[2,3-*c*]furan-1(3*H*)-one **6**, and CO (Table 2), which were the same species identified by Berreau and co-workers before[38] and were analogous to those produced upon irradiation of flavonol **2**.[34,35] In this study, it was essential to evaluate the photoreaction under the same conditions as those used in time-resolved spectroscopy studies. The maximum chemical yields of **5** and CO in irradiated aerated methanol solutions of **1** were 91 and 80%, respectively, which were the magnitudes comparable to those found for the photochemistry of **1** in acetonitrile.[38] In contrast, the yields of lactone **6** and CO formation in degassed samples were moderate (52−55%; Table 2). Lower chemical yields indicate competing photoreactions, but no other specific side products were identified by our analytical methods. The presence of oxygen alters the reaction mechanism, as is also supported by the labeling experiments of Berreau, providing evidence that

Table 1. Photophysical Properties of 1A and 1B in Methanol

compound	λ_{max}^{abs}/nm[a]	ε/(M^{-1} cm^{-1})[a]	λ_{max}^{em}/nm[b]	Φ_F[b]	τ_F/ns[b]
1A	344, 401	9720	472 (^{1}**1A***)	0.024 ± 0.004 (^{1}**1A***)	
			595 (^{1}**1Z***)	0.72 ± 0.06 (^{1}**1Z***)	5.1 ± 1.6
1B	472	10800	637	0.16 ± 0.01	3.2 ± 0.9
				0.15[c]	2.2[c]

[a] $c = 1 \times 10^{-4}$ M. [b] $c = 1 \times 10^{-5}$ M. [c] From ref 45.

https://dx.doi.org/10.1021/acs.joc.9b03248
J. Org. Chem. XXXX, XXX, XXX−XXX

Table 2. Photochemistry of 1 to Give Photoproducts 5 and 6

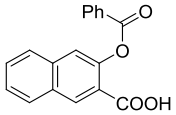

5

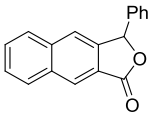

6

compound	$\Phi_r/10^{-2}$ [a]	yield of 5/% [b,c]	yield of 6/% [b,c]	yield of CO/% [b,c]	Φ_Σ [d]	Φ_Δ [e]
1A	3.1 ± 0.1 [b]	91 ± 8 [b]		80 ± 5 [b]	ineff	0.14 ± 0.01
	0.012 [c]		55 ± 5 [c]	52 ± 3 [c]		
	3.1 [e]					
1B	2.1 ± 0.1 [b]	55 ± 5 [b]		55 ± 3 [b]	0.26	0.07 ± 0.01
	0.00 [c]		30 ± 4 [c]	30 ± 4 [c]		
	0.28 [f]					

[a]The disappearance quantum yield of **1** ($c = 1 \times 10^{-4}$ M) upon direct irradiation. [b]Formation chemical yields of the corresponding photoproducts in aerated solutions. [c]Formation chemical yields of the corresponding photoproducts in degassed solutions. [d]The quantum yield of **1** disappearance in the presence of $^1O_2$ generated by excited rose bengal; ineff = inefficient. [e]The quantum yield of singlet-oxygen production from excited **1**. [f]The disappearance quantum yield measured in the presence of a large excess of a singlet-oxygen trap (furfuryl alcohol; 0.01 M).

Table 3. Photochemistry of 1A and 1B in Methanol[a]

compound	τ_S/ps [b]	k_{ISC}/s^{-1} [c]	Φ_{ISC} [d]	$\tau_T/\mu s$ [e,f]
1A	11 (^{1}**1Z***)	$(3.94 \pm 0.43) \times 10^9$	0.23 ± 0.02	0.1421 ± 0.0003 [e]
				1.630 ± 0.008 [f]
1B		$(3.47 \pm 0.21) \times 10^9$	n.d.	n.d. [e]
				0.0052 ± 0.0004 [f]

[a]Data obtained by TR spectroscopy measurements. [b]Singlet-state lifetime obtained by femtosecond spectroscopy. [c]The rate constant of ISC. [d]ISC quantum yield.[51] [e]Triplet-state lifetime obtained by nanosecond spectroscopy in aerated methanol solutions. [f]Triplet-state lifetime obtained by nanosecond spectroscopy in degassed methanol solutions.

the incorporated oxygen atoms in the product **5** originate from molecular oxygen.[38] The same photoproducts as those in the case of **1A** irradiation, including CO, were detected upon irradiation of both aerated and degassed methanol samples of **1B**, albeit the chemical yields were generally lower (Table 2). Such results were anticipated because Chou and co-workers identified the corresponding photoproducts upon irradiation of 3-hydroxyflavone **2B**.[35] Again, no other photoproducts were found in this case, and because the maximum CO yields match those of the related side products, we imply that the mass loss is related to different competing photoprocesses.

As we demonstrated above, the role of oxygen (O_2) in the kinetics of CO production from pure acid and base forms of **1** is significant. Although oxygen can act as a triplet-state quencher, it can also be a reagent (oxidant) in its ground ($^3O_2$) and excited (singlet oxygen, $^1O_2$) states. Therefore, we aimed our research to discriminate the individual effects of O_2 on the reaction.

Reaction with Singlet Oxygen. We used rose bengal (RB) as an auxiliary $^1O_2$ generator to learn whether the acid and base forms of **1** in the ground state can react with singlet oxygen. Irradiation of RB (λ_{irr} = 572 nm) in the presence of the acid **1A** in methanol resulted in a very inefficient (and incomplete) degradation even in a considerably prolonged experiment (16 h; Figure S22). On the contrary, the base **1B** disappeared within minutes under the same conditions (Figure S23). The quantum yield of **1B** disappearance, Φ_Σ = 0.26, demonstrated its high reactivity toward $^1O_2$. Using furfuryl alcohol (FFA; $k_\Sigma = 1.03 \times 10^8$ M^{-1} s^{-1}) and 1,3-diphenylisobenzofuran (DPBF; $k_\Sigma = 1.1 \times 10^9$ M^{-1} s^{-1})[46] as singlet-oxygen traps, we determined the rates of the reaction of both **1A** and **1B** with $^1O_2$ to be 4.3×10^5 and 4.7×10^8 M^{-1} s^{-1}, respectively.[47] For comparison, the conjugate base of parent flavonol **2B** was shown to react with $^1O_2$ in a basic aq solution with a similar rate constant of $k_\Sigma = 2.2 \times 10^8$ M^{-1} s^{-1}, whereas its conjugate acid **2A** was found to be only weakly reactive ($k_\Sigma = 2.5 \times 10^5$ M^{-1} s^{-1}).[35] In the presence of a large excess of FFA ($c = 1 \times 10^{-3}$ M), the Φ_r for **1A** remained unchanged, but it decreased by a factor of 7 for **1B** (Φ_r = from 2.1×10^{-2} to 2.8×10^{-3}; Table 2), which implies that the starting material was degraded by self-sensitized photooxygenation (see later). The maximum chemical yields of both **5** and CO produced from **1B** in the presence of $^1O_2$ were found to be ~60%, thus comparable to those obtained by direct irradiation of **1B** in aerated methanol.

Production of Singlet Oxygen. Singlet-oxygen production from the excited forms **1A** and **1B** is direct evidence for the involvement of their triplet excited states. Such a result would also be important for the CO production itself because $^1O_2$ hereby formed could subsequently react with the ground-state **1B** (and eventually inefficiently with **1A**), as demonstrated in the previous paragraph. The quantum yield of singlet-oxygen production (Φ_Δ) by triplet excited ^{3}**1A*** was determined using furfuryl alcohol (FFA) as a singlet-oxygen trap.[48] DPBF could not be used because of its significant spectral overlap with **1A**. Thus, a mixture of **1A** and FFA in aerated methanol was irradiated to complete conversion, and at the same time, **1A** was used as an actinometer because its Φ_r was determined independently (Table 2). The $^1O_2$ photoproduction was found to be relatively efficient, $\Phi_\Delta = 0.14 \pm 0.01$. Because **1A** was found essentially unreactive toward singlet oxygen, the self-sensitized photooxygenation pathway was excluded, and we concluded that $^1O_2$ produced by ^{3}**1A*** was not involved in the CO release from **1A** upon irradiation. The determination of Φ_Δ for **1B** was problematic because of its

https://dx.doi.org/10.1021/acs.joc.9b03248
J. Org. Chem. XXXX, XXX, XXX−XXX

high reactivity toward $^1O_2$ and thus a rapidly changing reaction composition (the absorbance of the irradiated solution). Therefore, a large excess of DPBF and short irradiation times were utilized to mitigate this issue. A solution of **1B** was irradiated at the tail of its absorption band at 507 nm, and the $^1O_2$ production quantum yield of Φ_Δ = 0.07 ± 0.01 was obtained (Table 2).

Time-Resolved Spectroscopy. Time-resolved (TR) spectroscopy was used to identify short-lived reaction intermediates produced from both **1A** and **1B** and to determine rate constants of the elementary reaction steps.

Nanosecond time-resolved spectroscopy of **1A** in aerated methanol ($c \sim 10^{-4}$ M; λ_{exc} = 355 nm; **1A** has a strong absorption band at ~400 nm) revealed a transient signal with λ_{max} = 440 nm. The lifetime of this species was strongly dependent on the concentration of oxygen. The kinetic traces were fitted with a first-order rate law (the oxygen concentration in an aerated methanol solution at 20 °C is almost 30 times higher, ~2.2×10^{-3} M,[49] than that of **1A**) to provide the lifetime of 142 ns in aerated methanol (Table 3; Figure S28). The lifetimes in oxygen-saturated and degassed methanol were determined to be 56 ns and 1.63 μs, respectively. The triplet-state lifetime of parent flavonol **2A** measured in methylpentane of τ_T = 7.8 μs has been determined before.[50] We first attempted to assign the signal to either triplet excited ^{3}**1Z*** or ^{3}**1A***. In the latter case, ^{1}**1Z***, formed from ^{1}**1A*** *via* ESIPT (see above), would have to undergo a reverse proton transfer during intersystem crossing to give ^{3}**1A***. Furthermore, a fluorescence signal up to 20 ns after the excitation pulse (λ_{max} = 600 nm, Figure 4) was still detectable in these experiments, which is consistent with the relatively long fluorescence lifetime measured by a steady-state technique (τ_F = 5.1 ns; Table 1).

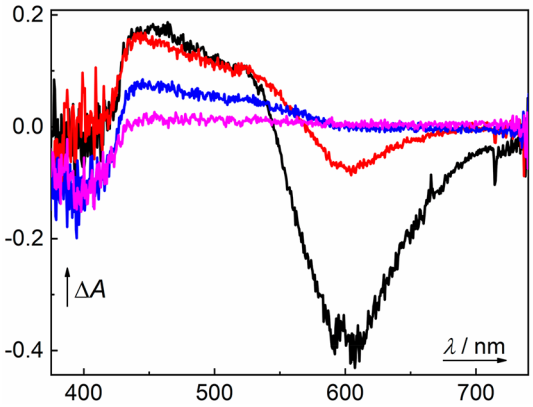

Figure 4. Transient absorption spectra of **1A** in aerated methanol (c = 8×10^{-5} M) taken after a 355 nm flash at different delay times (black = 10 ns, red = 20 ns, blue = 100 ns, magenta = 1 μs).

Nanosecond time-resolved spectroscopy of **1B** in both aerated and degassed methanol (λ_{exc} = 355 and 532 nm; **1B** has a strong absorption band at ~472 nm) did not show any signal of transient species (Figures S32, S33, and S34). We assumed that the ^{3}**1B*** lifetime is too short to be determined by our nanosecond equipment; therefore, a femtosecond pump-and-probe technique was used for its evaluation.

Femtosecond TR absorption experiments with a **1A** methanol solution (λ_{exc} = 387 nm) provided transient-absorption spectra, which possessed a signal with λ_{max} at 531 nm within 100 fs after the excitation (Figure 5). It was assigned to the singlet excited tautomer ^{1}**1Z***, generated rapidly from

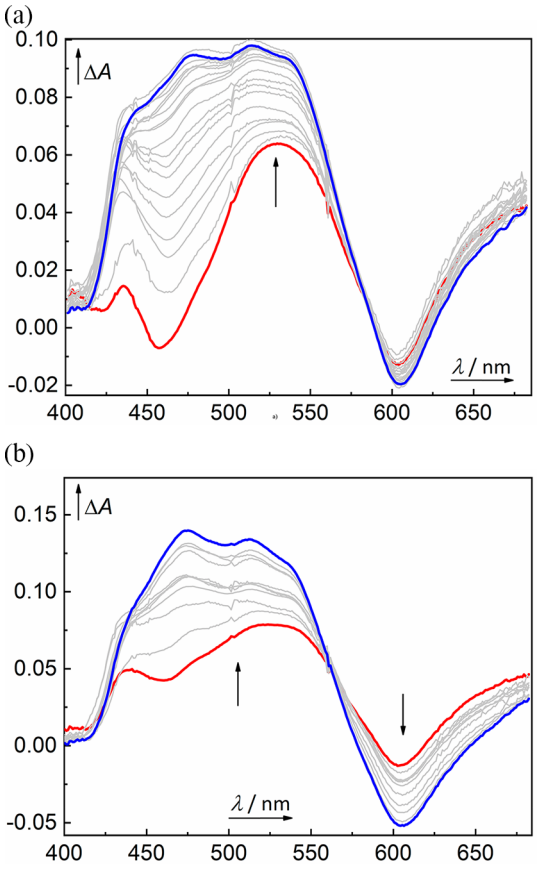

Figure 5. Femtosecond transient spectroscopy of **1A** ($c \sim 1.0 \times 10^{-3}$ M in methanol; excitation by a 387 nm laser pulse): (a) spectra obtained from 100 fs to 19 ps after the pulse; (b) spectra obtained from 5 to 500 ps after the pulse (initial state = red line; end state = blue line).

^{1}**1A*** (see above) *via* an analogous process observed for the excited tautomer of parent 3-hydroxyflavone **2**.[29] The corresponding decay kinetic data were fitted with a first-order rate law to provide the ^{1}**1Z*** lifetime of 11 ps (Table 3). In the case of parent 3-hydroxyflavone **2**, Harris and co-workers observed a fast ESIPT (240 fs) in nonpolar solvents, whereas the transfer was assumed to be much faster in methanol (<125 fs; faster than their instrument response).[29] The intersystem crossing rate constant of ^{1}**1Z*** to give triplet excited state ^{3}**1Z*** (λ_{max} at 440 nm), the species assigned by a ns TR spectroscopy, was $k_{ISC} = (3.94 \pm 0.43) \times 10^9$ s^{-1} (Table 3).

The femtosecond spectroscopy of **1B** in methanol (λ_{exc} = 475 nm) provided quite different results from those of **1A** because the compound cannot undergo ESIPT. The first signal with λ_{max} = 543 nm was assigned to the excited singlet state ^{1}**1B***. Its depletion with concomitant formation of a new band with λ_{max} = 549 nm was attributed to intersystem crossing and the new transient to ^{3}**1B*** (Figure 6). The kinetic traces were fitted by a first-order rate law to give the rate constant of (3.47 ± 0.21) × 10^9 s^{-1}, representing the rate constant of the triplet-state formation.

DFT Calculations for 1A and 1Z. We calculated the absorption maxima and excited-state energies for species **1A**

https://dx.doi.org/10.1021/acs.joc.9b03248
J. Org. Chem. XXXX, XXX, XXX−XXX

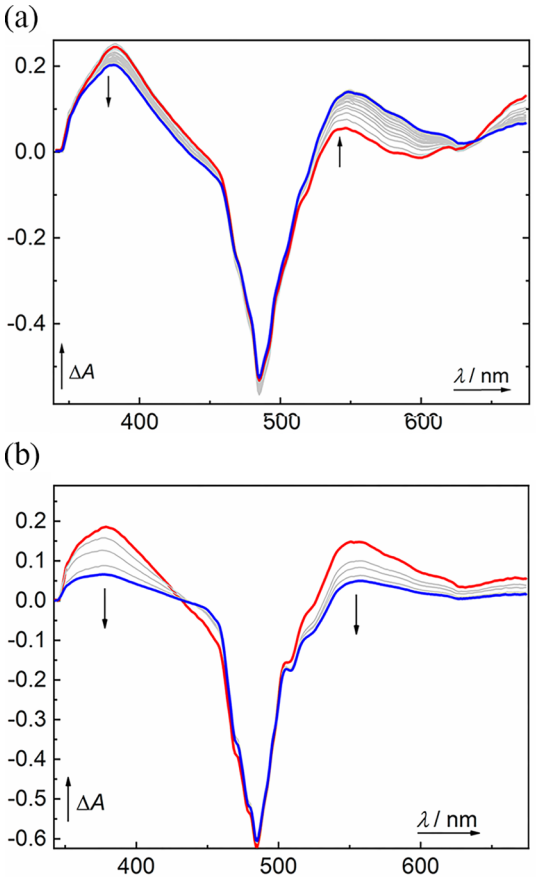

Figure 6. Femtosecond transient spectroscopy of **1B** ($c \sim 1.0 \times 10^{-3}$ M in methanol; excitation by a 475 nm laser pulse: (a) spectra obtained from 1 to 20 ps after the pulse; (b) spectra obtained from 3 ps to 3.1 ns (initial state = red line; end state = blue line).

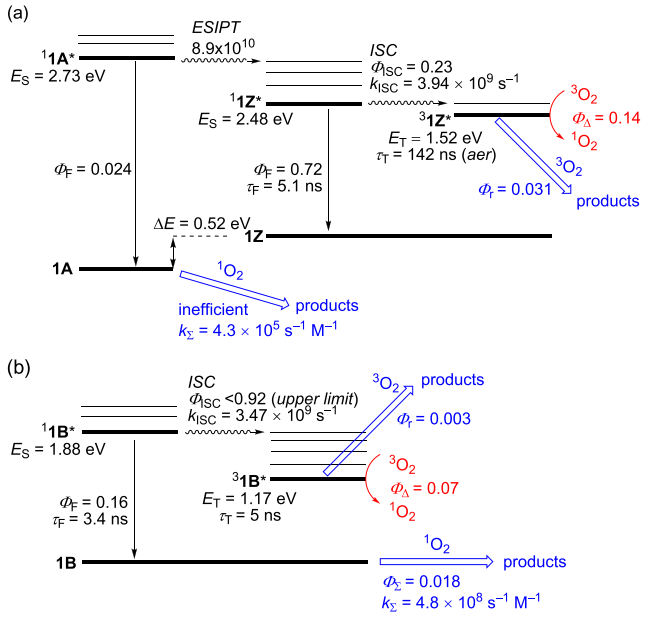

Figure 7. Jabłoński diagrams of (a) **1A** and (b) **1B** photochemistry in aerated (aer) methanol solutions. The adiabatic-state energies were calculated.

and **1Z** at the DFT level employing a B3LYP functional. The ground-state energy of **1A** was found to be lower than that of **1Z** by 0.52 eV (11.98 kcal mol^{-1}), which has also been reported for 3-hydroxyflavone **2A** (Figure 7).[52] The calculated excitation energies (Table S2) of first two excited states were 2.985 and 3.532 eV (f = 0.21 and 0.28 for S_1 and S_2 states, respectively), which is in very good agreement with the observed maxima of ~3.1 and 3.6 eV (401 and 344 nm, respectively; Table 1). The calculations of the S_1 excited-state minima for both ^{1}**1A*** and ^{1}**1Z*** resulted in stable structures (Table S3); the latter conformer is more stable by 0.26 eV (Tables S3 and S5). The calculated emission wavelengths of 481 and 670 nm for ^{1}**1A*** and ^{1}**1Z***, respectively, are in good harmony with the experimental values of 472 and 595 nm (Table 1), and they support the assignment of the ESIPT process responsible for the formation of ^{1}**1Z***. In addition, we evaluated the relative triplet energies of species ^{3}**1A*** and ^{3}**1Z***, showing that the latter zwitterionic state is lower in energy by 0.48 eV (Table S4). This allowed us to support our conclusions that the observed triplet excited state is the tautomer ^{3}**1Z***. The vertical $T_1 \rightarrow T_n$ (n = 2−6) transition energies were calculated to compare them with those found by our transient spectroscopy. The $T_1 \rightarrow T_3/T_4/T_5/T_6$ values for ^{3}**1Z*** of 529, 526, 490, and 465 nm (Table S4), respectively, could be assigned to the bands in the region of 450−550 nm (Figure 4).

DFT Calculations for 1B. We also calculated the vertical excitation energies of three lowest excited states of **1B** (Table S2), which gives the transition energies at 2.127 eV (583 nm), 2.852 eV (435 nm), and 3.236 eV (383 nm). Contrary to the results for **1A**, these calculations gave larger errors when compared to the experimental data; in particular, the absorption energy of the lowest excited state was lower by ~0.5 eV. Such an underestimation of the absorption energies of an anionic form has also been observed for 3-hydroxyflavone.[53] The excited-state ^{1}**1B*** relaxes to its minimum at 1.878 eV above the ground-state minimum (Table S3), and the predicted emission energy from this state at 717 nm compares reasonably well to the experimental value of 637 nm (Table 1 and Table S3). These data are in accord with those obtained for 3-hydroxyflavone **2**.[52] The corresponding triplet-state ^{3}**1B*** was found lower in energy than that of ^{1}**1B*** by 0.706 eV.

Photorelease Mechanism. Our experimental results showed that the triplet excited state formed from **1A** must exclusively be responsible for the formation of CO and photoproducts. Upon irradiation, **1A** in a methanol solution is excited to its singlet excited state ^{1}**1A***, which is converted to excited phototautomer ^{1}**1Z*** in less than 100 fs. This species is highly fluorescent; the total emission quantum yield from both excited tautomers is ~0.74 ($\Phi_F(^1\mathbf{1Z}^*) = 0.72$; Table 1). The subsequent fast ^{3}**1Z*** formation ($k_{ISC} = (3.9 \pm 0.4) \times 10^9$ s^{-1}) is efficient ($\Phi_{ISC} = 0.23$; Table 3). The photoreaction quantum yield (Φ_r) of 0.03 found for aerated solutions is related to the formation of CO and naphthoic acid derivative **5** as the exclusive photoproducts obtained from ^{3}**1Z***. This species also sensitizes oxygen to form $^1O_2$ with $\Phi_\Delta = 0.14$ (Table 2) under the given experimental conditions (the initial O_2 concentration in methanol is ~2.2 × 10^{-3} M[49]). The remaining triplet undergoes intersystem crossing to give the ground-state tautomer, which slowly regenerates[36] the starting material **1A**. The Φ_r value did not change in the presence of a large excess of FFA as a $^1O_2$ trap (Table 2); thus singlet oxygen,

https://dx.doi.org/10.1021/acs.joc.9b03248
J. Org. Chem. XXXX, XXX, XXX−XXX

produced by ^{3}**1Z*** sensitization, cannot be responsible for the formation of the photoproducts. The reaction of ^{3}**1Z*** with ground-state oxygen ($^3O_2$) is a spin-allowed process; in contrast, the ground-state (normal form) **1A** reacts with $^1O_2$ very slowly and inefficiently. The only detected photoproducts, **5** and CO, are formed in very high chemical yields; no detectable amounts of photoproduct **6** were found in aerated solutions. The mechanism of the final photooxygenation step has been a subject of investigations with parent flavonol **2**.[32−35,38,53−56] Chou and co-workers proposed that the reaction of triplet phototautomer ^{3}**2Z*** with ground-state oxygen takes place *via* the formation of an endoperoxide intermediate.[35,53−55] Recent DFT calculations by Kubinyi and co-workers gave evidence that the addition of $^3O_2$ on ^{3}**2Z*** gives an endoperoxide and not a hydroperoxide as an intermediate.[57] Inspired by these studies, we show an analogous endoperoxide intermediate **7**, formed upon the reaction of ^{3}**1Z*** with ground-state oxygen, in Scheme 3a; the previously studied mechanism of **2Z** photooxygenation is provided in Scheme S1. We conclude that the reaction of ^{3}**1Z*** with $^3O_2$ is a nearly exclusive pathway leading to these photoproducts and that sensitization of oxygen by ^{3}**1Z*** is a nonproductive process. Figure 7a shows a Jabłoński diagram constructed from all our experimental and computational data.

Scheme 3. Major Reaction Pathways in the Photochemistry of (a) 1A and (b) 1B under Aerobic (Red) and Anaerobic (Blue) Conditions in Methanol

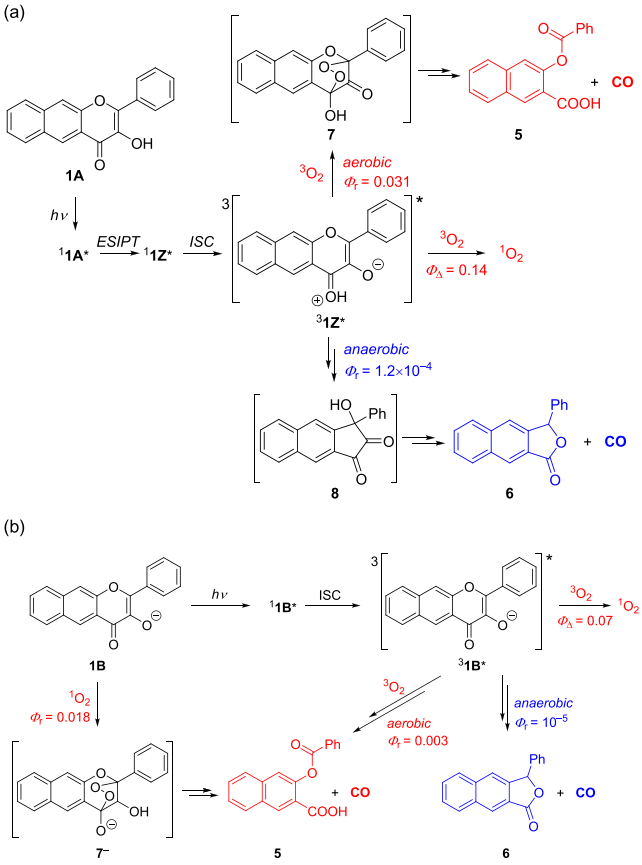

Upon irradiation of **1A** in a degassed methanol, the first fast steps of the mechanism are identical to those of **1A** in an aerated solution. Upon the formation of triplet excited[34] ^{3}**1Z***, the compound undergoes a very inefficient (Φ_r = 1.2 × 10^{-4}) rearrangement to give lactone **6** as the only identified side product (Scheme 3b). This reaction most probably proceeds *via* an intermediate **8**, proposed by Yokoe[58] and computationally predicted by Kubinyi[57] and their co-workers in the case of 3-hydroxyflavone **2** (Scheme S1). Because the oxygen sensitization pathway is not available and the reaction quantum yield is insignificant, ^{3}**1Z*** must efficiently regenerate the starting material or be destroyed *via* an even less efficient chemical process. This reaction pathway represents an unimportant side process in the overall mechanism, and it is not observed in aerated solutions.

The photochemistry of **1B** is fundamentally different from that of **1A** because it cannot undergo phototautomerization. The singlet excited state ^{1}**1B*** is only weakly fluorescent (Φ_F = 0.16; τ_F = 3.4 ns), and it is rapidly ((3.47 ± 0.21) × 10^9 s^{-1}; Table 1) converted to its triplet state (^{3}**1B***). Unfortunately, we were unable to determine Φ_{ISC} because its lifetime was too short to be detected by our nanosecond LFP apparatus, but we estimated an upper limit for Φ_{ISC} to be as high as 0.92 (thus, a radiationless decay for ^{1}**1B*** is negligible). The triplet excited ^{3}**1B*** sensitizes oxygen with Φ_Δ = 0.07 (Table 2). The irradiation of **1B** in aerated methanol gives the same photoproducts (**5** and CO) as that of **1A** with a similar efficiency (Φ_r = 2.1 × 10^{-2}) but lower maximum chemical yields (55%). Thus, the triplet and probably singlet excited states must undergo an efficient radiationless decay to regenerate the starting material. The stark difference between the photochemistry of **1A** and **1B** is represented by the contrasting reactivity with singlet oxygen. **1B** reacts more efficiently with $^1O_2$ (Φ_Σ = 0.26; Table 2) than **1A** by more than 3 orders of magnitude, presumably because the addition of electrophilic $^1O_2$ onto the electron-rich anion core of the ground state of **1B** is favorable. The Φ_Σ value of 2.0 × 10^{-2} for **1B** calculated from Φ_Δ, the bimolecular reaction rate of **1B** with $^1O_2$ (k_Σ), and the rate constant of $^1O_2$ decay (k_d) using a steady-state approximation (see Supporting Information) is comparable to the experimentally determined value of Φ_r = (2.1 ± 0.1) × 10^{-2} found for direct irradiation of **1B**. At the same time, we demonstrated that the chemical yield of CO was unaffected by the type of reaction initiation (direct irradiation versus RB sensitization). In an important experiment, the Φ_r value considerably decreased in the presence of a large excess of FFA as an $^1O_2$ trap (Table 2). The Φ_r decrease from 2.1 × 10^{-2} to 2.8 × 10^{-3} (Table 2) provides an inherent quantum yield for the reaction of **1B** with $^1O_2$ under the given conditions (**1B** and O_2 concentrations in the sample), thus (2.1 × 10^{-2}) − (2.8 × 10^{-3}) gives Φ_r of ∼1.8 × 10^{-2}. The Φ_r value of 2.8 × 10^{-3} must be related to the reaction of the triplet ^{3}**1B*** with ground-state oxygen (O_2), representing the efficiency as still 2 orders of magnitude larger than that of the reaction under anaerobic conditions. Therefore, CO and acid **5** are not formed exclusively by the reaction of ground-state **1B** with $^1O_2$ generated by self-sensitization. The mechanism of the photooxygenation of 3-hydroxyflavone **2B** has also been suggested to proceed *via* an endoperoxide intermediate by Chou and co-workers (Supporting Information),[54] analogous to species **7** shown in Scheme 3b. The Jabłoński diagram for the **1B** photochemistry is shown in Figure 7b.

In the absence of oxygen, the formation of naphthoic acid derivative **5** from ^{3}**1B*** is not observed; instead, CO and lactone **6** are produced very inefficiently (Φ_r ∼ 10^{-5}). These photoproducts suggest a similar reaction pathway to that of

https://dx.doi.org/10.1021/acs.joc.9b03248
J. Org. Chem. XXXX, XXX, XXX−XXX

^{3}**1A***. This reaction is again insignificant in the overall phototransformation.

In the case of a mixture of **1A** and **1B** that forms at different solution pHs, we have a collection of three major reaction pathways involving both forms, all of which lead to CO formation but with considerably different efficiencies and oxygen demands, but only if both forms can be excited. The common denominator for these processes is the triplet multiplicity of the productive excited state. The presence of two orthogonal reaction pathways for **1A** and **1B** thus implies additional considerations for solutions where the concentrations of both species vary. The same photoproducts, **5** and CO, will be produced by the reactions of triplet excited intermediates ^{3}**1Z*** and ^{3}**1B*** with $^3O_2$, whereas **1B** will be substantially depleted by oxygenation with $^1O_2$. Considering just an acid−base equilibrium, the amount of CO generated from **1B** will increase with increasing acidity of the 3-hydroxyflavone analogue or increasing pH of the solution. It will also be strongly dependent on the emission spectrum of an irradiation source due to considerably different absorption spectra of both acid−base forms. Although other side reactions may always compete (Table 2), they represent only a negligible sink.

CONCLUSIONS

Our experimental results revealed a reaction dichotomy of acid−base forms of 3-hydroxy-2-phenyl-4*H*-chromen-4-one, **1A** and **1B**, manifested by three major orthogonal decarbonylation pathways, which impose serious ramifications for the future development of novel 3-hydroxyflavone-based photoCORMs. The reaction of the triplet excited tautomer of the conjugate acid **1A**, ^{3}**1Z***, with $^3O_2$ is a nearly exclusive reaction pathway leading to the release of CO and photoproducts, whereas **1A** is nearly unreactive toward singlet oxygen, produced from ^{3}**1Z*** sensitization as a side product. On the contrary, the conjugate base **1B** provides CO *via* an efficient oxygenation reaction with singlet oxygen formed by sensitization of ^{3}**1B***; therefore, the major CO-releasing pathway is a self-sensitized photooxygenation. CO can also be liberated by very inefficient photorearrangements of both ^{3}**1Z*** and ^{3}**1B***.

Because the triplet excited states have been established as productive states, increasing the quantum yield of intersystem crossing is desirable to improve the efficacy of the CO liberation. The intramolecular reaction rate of **1B** with $^1O_2$, which is an order of magnitude below the diffusion limits, brings another chance to significantly improve the CO release quantum yield. Most importantly, **1B** might also serve as an attractive lead structure to achieve CO release using light in the near-infrared region by harnessing its high affinity toward $^1O_2$. Schnermann has shown such an application in self-sensitized photooxidation of near-infrared light-activated cyanine photocages and demonstrated the feasibility of this approach for targeted *in vivo* delivery.[59,60] The understanding of the mechanism will guide future endeavors to improve the CO release efficiency by 3-hydroxyflavone chromophores modifications and may help in their potential medical applications as photoCORMs.

EXPERIMENTAL SECTION

Materials and Methods. Reagents and solvents of the highest purity available were used as purchased, or they were purified/dried using standard methods when necessary. The compounds **1**, **5**, and **6** were synthesized according to the published procedures.[20,38,61,62]

Absorption spectra and the molar absorption coefficients were obtained on a UV−vis spectrometer with matched 1.0 cm quartz cells. Molar absorption coefficients were determined from the absorption spectra (the average values were obtained from three independent measurements with solutions of different concentrations). Fluorescence was measured on an automated luminescence spectrometer in 1.0 cm quartz fluorescence cuvettes at 23 ± 1 °C. The corresponding optical filters were used to avoid the second harmonic excitation/emission bands induced by the grating. The samples of concentration with the absorbance of ∼0.1 at the excitation wavelength were used. Each sample was measured five times, and the spectra were averaged. Emission and excitation spectra are normalized. Fluorescence quantum yields were determined using an integration sphere as the absolute values. For each sample, the quantum yield was measured five times and then it was averaged. ^{1}H NMR spectra were recorded on 300 or 500 MHz spectrometers; ^{13}C NMR spectra were obtained on 125 or 75 MHz instruments in $CDCl_3$, CD_3OD, and D_2O. ^{1}H chemical shifts are reported in ppm relative to tetramethylsilane (δ = 0.00 ppm) using the residual solvent signal as an internal reference. ^{13}C chemical shifts are reported in ppm with $CDCl_3$ (δ = 77.67 ppm) and CD_3OD (δ = 49.30 ppm) as internal references. Deuterated solvents were kept under a nitrogen atmosphere. The exact masses of the synthesized compounds were obtained using a triple quadrupole electrospray ionization mass spectrometer in a positive or negative mode coupled with direct-inlet or liquid chromatography.

Spectrophotometric Determination of pK_a. A freshly prepared solution of **1A** ($c \sim 8.5 \times 10^{-5}$ M) in DMSO/H_2O (1:1; 2.5 mL, I = 0.1 M) was transferred into a matched 1.0 cm quartz cuvette and its UV−vis absorption spectrum was recorded. The solution was basified by the addition of small aliquots of aq NaOH (typically 10 μL; 0.5 and 0.1 M), and the pH and UV−vis absorption spectra were recorded after each addition. Volume changes in the titration were corrected. The pK_a value was determined by deconvolution using a multivariate analysis.

General Procedure for Irradiation in UV Cuvettes. A solution of a compound in the given solvent (3 mL) in a matched 1.0 cm quartz PTFE screw-cap cuvette equipped with a stirring bar was stirred and irradiated with a light source of 32 LEDs (λ_{irr} = 405 and 450 nm; Figure S37). The progress of the reactions was monitored at the given time intervals by UV−vis spectrometry using a diode-array spectrophotometer. In some experiments, light pulses (425.6 Hz repetition rate, ≤150 fs pulse length, and energy of ∼7.5 ± 0.3 mW) from a Ti:sapphire laser coupled to a noncollinear optical parametric amplifier (NOPA) with the wavelength set to 505 nm (fwhm ∼15 nm) were used to irradiate the samples.

Fluorescence Measurements. Fluorescence and excitation spectra were measured using a fluorescence spectrometer in a 1.0 cm quartz fluorescence cuvette at 23 ± 1 °C. The sample concentrations were adjusted to keep the absorbance below 0.2 at the corresponding excitation wavelength. Each sample was measured five times, and the spectra were averaged. Emission and excitation spectra were normalized and corrected by the photomultiplier sensitivity function using correction files supplied by the manufacturer.

Decomposition Quantum Yield Determination. The decomposition quantum yields of **1A** in an aerated methanol solution were determined using ferrioxalate ($c = 1.0 \times 10^{-5}$ M) in aqueous phosphate buffered saline (PBS, I = 0.1 M, pH = 7.4) as an actinometer, using a Xe lamp fitted with a monochromator (λ_{irr} = 400 ± 2 nm). The subsequent quantum yields of decomposition were determined relative to **1A** using an LED source (λ_{irr} = 405 or 420 nm; Figure S37).

Singlet-Oxygen Production Quantum Yields. A solution of 1,3-diphenylisobenzofuran (DPBF; $c = 1 \times 10^{-4}$) and either **1B** ($c = 5 \times 10^{-5}$ M) or rose bengal (RB) as sensitizers ($c = 5 \times 10^{-6}$ M) in methanol was prepared. The stirred solution (3.5 mL) in a quartz cell (1 cm) was irradiated using LEDs at 507 nm, and the UV−vis spectra were recorded periodically. The irradiation period was selected to reach around 10% conversion of DPBF. The procedure was repeated five times. The decomposition of DPBF monitored at 411 nm was

https://dx.doi.org/10.1021/acs.joc.9b03248
J. Org. Chem. XXXX, XXX, XXX−XXX

fitted with a pseudo-first-order rate law, and the singlet-oxygen formation quantum yield Φ_Δ was calculated using RB as the reference (Φ_Δ = 0.76[63]).

A methanol solution containing furfuryl alcohol ($c = 1.0 \times 10^{-3}$ M) and **1A** ($c = 1.0 \times 10^{-4}$ M) was stirred and irradiated using LEDs at 405 nm until the **1A** disappearance was complete. The amount of FFA consumed by singlet oxygen was determined by HPLC using a reported method.[48] The quantum yield of the singlet-oxygen production was calculated from Φ_r of **1A** and a bimolecular rate constant of the reaction of FFA with $^1O_2$ in methanol ($k_r = 1.03 \times 10^8$ M^{-1} s^{-1}).

Reaction of 1A and 1B with $^1O_2$. Solutions containing 1,3-diphenylisobenzofuran (DPBF; $c = 2 \times 10^{-4}$ M), **1A** ($c = 1 \times 10^{-4}$ M) or **1B** ($c = 1 \times 10^{-4}$ M), and RB ($c = 5 \times 10^{-6}$ M) as a singlet-oxygen sensitizer in methanol were prepared. A stirred solution (3.5 mL) in a quartz cell (1.0 cm) was irradiated with an LED at 590 nm (Figure S37), and UV−vis absorption spectra were recorded at the given intervals. The rate constant of DPBF and of the **1A** and **1B** decompositions were determined from the decay at the corresponding absorption maxima (λ_{max}). The bimolecular reaction rates of the reaction of **1A** or **1B** with $^1O_2$ were calculated using the known rate constant of singlet oxygen quenching in methanol ($k_d = 9 \times 10^4$ s^{-1}) and the bimolecular reaction rate constant of DPBF with singlet oxygen ($k_r = 1.2 \times 10^9$ M^{-1} s^{-1}).[46]

Determination of the Photoproducts. A solution of **1A** or **1B** (3.5 mL, $c \sim 1 \times 10^{-4}$ M, methanol) in a quartz cuvette was irradiated with LEDs at 405 or 450 nm to complete conversion. The resulting mixture was analyzed by HPLC (with a reversed-phase column and a mixture of methanol and water (with 0.1% formic acid) with a different gradient used as eluent; 1 mL min^{-1}). The photoproducts as analytical standards were prepared independently by known synthetic routes (**5**,[20,38] **6**[61]) to unequivocally establish the structure of the photoproducts.

Determination of CO Yield. A solution of **1A** or **1B** (500 μL, $c \sim 1 \times 10^{-4}$ M, in methanol) was irradiated with LEDs at 405 or 450 nm in closed GC vials fitted with PTFE septa to complete conversion. The released CO was analyzed and quantified by a GC-headspace technique, which was calibrated using the photoreaction of cyclopropenone photoCORM[14] (50−500 μL, $c \sim 5 \times 10^{-4}$ M, in methanol).

Transient Spectroscopy. The LFP nanosecond setup was generally operated in a right-angle arrangement of the pump and probe beams. Laser pulses of ≤170 or 700 ps duration at 355 nm (20−180 mJ) were obtained from a Nd:YAG laser. The laser beam was dispersed onto a 40 mm long and 10 mm wide modified fluorescence cuvette held in a laying arrangement. An overpulsed Xe arc lamp was used as the source of the probe light. Kinetic traces were recorded using a photomultiplier. Transient absorption spectra were obtained using an ICCD camera equipped with a spectrograph. The samples were degassed by three freeze−pump−thaw cycles under reduced pressure (0.04 Torr). Absorption spectra of the sample solutions were measured regularly between laser flashes to test for possible photodegradation of the solution components using a diode-array spectrophotometer.[64]

Femtosecond transient absorption was measured with the pump−supercontinuum probe technique using a Ti/Sa laser system (775 nm, pulse energy 0.9 mJ, full width at half-maximum 150 fs, operating frequency 426 Hz). Part of the beam was fed into a noncollinear optical parametric amplifier (NOPA). The output at 387 nm (for **1A**) and 470 nm (for **1B**) was frequency-doubled by a β-barium borate (BBO) crystal to λ = 266 nm and, upon compression, elicited pump pulses of 1 μJ energy and <150 fs pulse width. The probe beam was generated by focusing the 775 nm beam in front of a CaF_2 plate with a 2 mm path length that produced a supercontinuum spanning a wavelength range of 270−690 nm. The pump and probe beams were focused to a 0.2 mm spot on the sample that was flowing in an optical cell with a thickness of 0.4 mm. The probe beam and a reference signal obtained by passing the solution next to the pump beam were spectrally dispersed and registered with two photodiode arrays (512 pixels). Transient absorption spectra were calculated from the ratio of the two beams. The pump−probe cross-correlation was <100 fs over the entire spectrum. The measurements were performed at ambient temperature (20 ± 2 °C). The kinetic traces were fitted by single or multiple exponential decay functions. In the case of the second-order kinetics, the corresponding differential equations were solved using the Levenberg−Marquard minimization algorithm.[64]

Quantum Chemical Calculations. The calculations of ground, singlet (S_1), and triplet (T_1) excited state minima have been performed with the clusters that consisted of **1A**, **1Z**, and **1B** species and one methanol molecule explicitly included in the quantum mechanical description to account specifically for the proton transfer in both ground and excited states. The additional solvent effects have been modeled for by means of the polarizable continuum model (PCM).[65] The calculations were carried out at the DFT level employing a B3LYP functional;[66,67] a TD approach was used in the calculations of the excited states.[68,69] All calculations were performed with a TZVP basis set.[70,71] The same level of theory was also used for calculations of all absorption spectra. The Gaussian 16 program package was used for the calculations.[72]

■ ASSOCIATED CONTENT

Supporting Information

The Supporting Information is available free of charge at https://pubs.acs.org/doi/10.1021/acs.joc.9b03248.

Figures of NMR spectra, determination of pK_a, UV−vis absorption spectra, emission spectra, irradiation spectra, HPLC spectra and calibrations, HPLC−HRMS analysis, transient absorption spectra, kinetic decay, picosecond LPF, heat maps, and normalized emission spectra, equations of quantum-yield calculations, tables of ISC quantum yields, calculated vertical excitation energies, wavelengths, and oscillator strengths, calculated adiabatic energies, and structures for compounds, and schemes of photochemistry under aerobic and anaerobic conditions (PDF)

■ AUTHOR INFORMATION

Corresponding Author

Petr Klán − *Department of Chemistry and RECETOX, Masaryk University, 625 00 Brno, Czech Republic;* orcid.org/0000-0001-6287-2742; Phone: +420-54949-4856; Email: klan@sci.muni.cz; Fax: +420-54949-2443

Authors

Marina Russo − *Department of Chemistry and RECETOX, Masaryk University, 625 00 Brno, Czech Republic*

Peter Šťacko − *Department of Chemistry and RECETOX, Masaryk University, 625 00 Brno, Czech Republic*

Dana Nachtigallová − *Institute of Organic Chemistry and Biochemistry, 16610 Prague, Czech Republic;* orcid.org/0000-0002-9588-8625

Complete contact information is available at: https://pubs.acs.org/10.1021/acs.joc.9b03248

Notes

The authors declare no competing financial interest.

■ ACKNOWLEDGMENTS

Support for this work was provided by the Czech Science Foundation (GA18-12477S) and also by the Czech Ministry of Education, Youth and Sports (the RECETOX research infrastructure: LM2018121 and the CETOCOEN EXCELLENCE Teaming 2 project: 02.1.01/0.0/0.0/18_046/0015975). We thank Luboš Jílek and Vojtěch Orel (Masaryk

https://dx.doi.org/10.1021/acs.joc.9b03248
J. Org. Chem. XXXX, XXX, XXX−XXX

University) for their help with the experiments, Jakob Wirz (University of Basel) for fruitful discussions, and Miroslava Bittová (Masaryk University) for HRMS analyses. This work was also a part of the research project RVO (61388963) of the IOCB of the Czech Academy of Sciences (D.N.).

REFERENCES

(1) Weaver, L. K. Carbon monoxide poisoning. *Crit. Care Clin.* **1999**, *15*, 297.
(2) Wu, L.; Wang, R. Carbon monoxide: endogenous production, physiological functions, and pharmacological applications. *Pharmacol. Rev.* **2005**, *57*, 585.
(3) Lowson, S. M. Alternatives to nitric oxide. *Br. Med. Bull.* **2004**, *70*, 119.
(4) Otterbein, L. E.; Otterbein, S. L.; Ifedigbo, E.; Liu, F.; Morse, D. E.; Fearns, C.; Ulevitch, R. J.; Knickelbein, R.; Flavell, R. A.; Choi, A. M. MKK3 mitogen-activated protein kinase pathway mediates carbon monoxide-induced protection against oxidant-induced lung injury. *Am. J. Pathol.* **2003**, *163*, 2555.
(5) Nguyen, D.; Nguyen, T.-K.; Rice, S. A.; Boyer, C. CO-releasing polymers exert antimicrobial activity. *Biomacromolecules* **2015**, *16*, 2776.
(6) Romao, C. C.; Blättler, W. A.; Seixas, J. D.; Bernardes, G. J. Developing drug molecules for therapy with carbon monoxide. *Chem. Soc. Rev.* **2012**, *41*, 3571.
(7) Weinhouse, S.; Warburg, O.; Burk, D.; Schade, A. L. On respiratory impairment in cancer cells. *Science* **1956**, *124*, 267.
(8) Wegiel, B.; Gallo, D.; Csizmadia, E.; Harris, C.; Belcher, J.; Vercellotti, G. M.; Penacho, N.; Seth, P.; Sukhatme, V.; Ahmed, A. Carbon monoxide expedites metabolic exhaustion to inhibit tumor growth. *Cancer Res.* **2013**, *73*, 7009.
(9) Heinemann, S. H.; Hoshi, T.; Westerhausen, M.; Schiller, A. Carbon monoxide—physiology, detection and controlled release. *Chem. Commun.* **2014**, *50*, 3644.
(10) Üstün, E.; Ayvaz, M. C.; Çelebi, M. S.; Aşcı, G.; Demir, S.; Özdemir, İ. Structure, CO-releasing property, electrochemistry, DFT calculation, and antioxidant activity of benzimidazole derivative substituted $[Mn(CO)_3(bpy)L]PF_6$ type novel manganese complexes. *Inorg. Chim. Acta* **2016**, *450*, 182.
(11) Yempally, V.; Kyran, S. J.; Raju, R. K.; Fan, W. Y.; Brothers, E. N.; Darensbourg, D. J.; Bengali, A. A. Thermal and Photochemical Reactivity of Manganese Tricarbonyl and Tetracarbonyl Complexes with a Bulky Diazabutadiene Ligand. *Inorg. Chem.* **2014**, *53*, 4081.
(12) Anderson, S. N.; Larson, M. T.; Berreau, L. M. Solution or solid—it doesn't matter: visible light-induced CO release reactivity of zinc flavonolato complexes. *Dalton T.* **2016**, *45*, 14570.
(13) Southam, H. M.; Smith, T. W.; Lyon, R. L.; Liao, C.; Trevitt, C. R.; Middlemiss, L. A.; Cox, F. L.; Chapman, J. A.; El-Khamisy, S. F.; Hippler, M.; Williamson, M. P.; Henderson, P. J. F.; Poole, R. K. A thiol-reactive Ru(II) ion, not CO release, underlies the potent antimicrobial and cytotoxic properties of CO-releasing molecule-3. *Redox Biol.* **2018**, *18*, 114.
(14) Martinek, M.; Filipova, L.; Galeta, J.; Ludvikova, L.; Klan, P. Photochemical Formation of Dibenzosilacyclohept-4-yne for Cu-Free Click Chemistry with Azides and 1, 2, 4, 5-Tetrazines. *Org. Lett.* **2016**, *18*, 4892.
(15) Kuzmanich, G.; Garcia-Garibay, M. A. Ring strain release as a strategy to enable the singlet state photodecarbonylation of crystalline 1, 4-cyclobutanediones. *J. Phys. Org. Chem.* **2011**, *24*, 883.
(16) Chapman, O.; Wojtkowski, P.; Adam, W.; Rodriguez, O.; Rucktäschel, R. Photochemical transformations. XLIV. Cyclic peroxides. Synthesis and chemistry of. alpha.-lactones. *J. Am. Chem. Soc.* **1972**, *94*, 1365.
(17) Peng, P.; Wang, C.; Shi, Z.; Johns, V. K.; Ma, L.; Oyer, J.; Copik, A.; Igarashi, R.; Liao, Y. Visible-light activatable organic CO-releasing molecules (photoCORMs) that simultaneously generate fluorophores. *Org. Biomol. Chem.* **2013**, *11*, 6671.
(18) Antony, L. A. P.; Slanina, T.; Sebej, P.; Solomek, T.; Klan, P. Fluorescein analogue xanthene-9-carboxylic acid: a transition-metal-free CO releasing molecule activated by green light. *Org. Lett.* **2013**, *15*, 4552.
(19) Solomek, T.; Wirz, J.; Klan, P. Searching for Improved Photoreleasing Abilities of Organic Molecules. *Acc. Chem. Res.* **2015**, *48*, 3064.
(20) Popova, M.; Soboleva, T.; Arif, A. M.; Berreau, L. M. Properties of a flavonol-based photoCORM in aqueous buffered solutions: influence of metal ions, surfactants and proteins on visible light-induced CO release. *RSC Adv.* **2017**, *7*, 21997.
(21) Grubel, K.; Laughlin, B. J.; Maltais, T. R.; Smith, R. C.; Arif, A. M.; Berreau, L. M. Photochemically-induced dioxygenase-type CO-release reactivity of group 12 metal flavonolate complexes. *Chem. Commun.* **2011**, *47*, 10431.
(22) Griffiths, H. R.; Gao, D.; Pararasa, C. Redox regulation in metabolic programming and inflammation. *Redox Biol.* **2017**, *12*, 50.
(23) Holmström, K. M.; Finkel, T. Cellular mechanisms and physiological consequences of redox-dependent signalling. *Nat. Rev. Mol. Cell Biol.* **2014**, *15*, 411.
(24) Banerjee, R. Redox outside the box: linking extracellular redox remodeling with intracellular redox metabolism. *J. Biol. Chem.* **2012**, *287*, 4397.
(25) Fetzner, S. Ring-cleaving dioxygenases with a cupin fold. *Appl. Environ. Microbiol.* **2012**, *78*, 2505.
(26) Sokolová, R.; Ramešová, Š.; Degano, I.; Hromadová, M.; Gál, M.; Žabka, J. The oxidation of natural flavonoid quercetin. *Chem. Commun.* **2012**, *48*, 3433.
(27) Zenkevich, I.; Eshchenko, A.; Makarova, S.; Vitenberg, A.; Dobryakov, Y.; Utsal, V. Identification of the products of oxidation of quercetin by air oxygenat ambient temperature. *Molecules* **2007**, *12*, 654.
(28) Sengupta, P. K.; Kasha, M. Excited state proton-transfer spectroscopy of 3-hydroxyflavone and quercetin. *Chem. Phys. Lett.* **1979**, *68*, 382.
(29) Schwartz, B. J.; Peteanu, L. A.; Harris, C. B. Direct observation of fast proton transfer: femtosecond photophysics of 3-hydroxyflavone. *J. Phys. Chem.* **1992**, *96*, 3591.
(30) Dick, B.; Ernsting, N. P. Excited-state intramolecular proton transfer in 3-hydroxylflavone isolated in solid argon: fluoroescence and fluorescence-excitation spectra and tautomer fluorescence rise time. *J. Phys. Chem.* **1987**, *91*, 4261.
(31) Soboleva, T.; Esquer, H. J.; Benninghoff, A. D.; Berreau, L. M. Sense and release: a thiol-responsive flavonol-based photonically driven carbon monoxide-releasing molecule that operates via a multiple-input AND logic gate. *J. Am. Chem. Soc.* **2017**, *139*, 9435.
(32) Matsuura, T.; Matsushima, H.; Sakamoto, H. Photosensitized oxygenation of 3-hydroxyflavones. Possible model for biological oxygenation. *J. Am. Chem. Soc.* **1967**, *89*, 6370.
(33) Matsuura, T.; Matsushima, H.; Nakashima, R. Photoinduced reactions—XXXVI: Photosensitized oxygenation of 3-hydroxyflavones as a nonenzymatic model for quercetinase. *Tetrahedron* **1970**, *26*, 435.
(34) Matsuura, T.; Takemoto, T.; Nakashima, R. Photoinduced reactions—LXXI: Photorearrangement of 3-hydroxyflavones to 3-aryl-3-hydroxy-1, 2-indandiones. *Tetrahedron* **1973**, *29*, 3337.
(35) Studer, S. L.; Brewer, W. E.; Martinez, M. L.; Chou, P. T. Time-resolved study of the photooxygenation of 3-hydroxyflavone. *J. Am. Chem. Soc.* **1989**, *111*, 7643.
(36) Martinez, M. L.; Studer, S. L.; Chou, P. T. Direct evidence of the triplet-state origin of the slow reverse proton transfer reaction of 3-hydroxyflavone. *J. Am. Chem. Soc.* **1990**, *112*, 2427.
(37) Popova, M.; Soboleva, T.; Ayad, S.; Benninghoff, A. D.; Berreau, L. M. Visible-light-activated quinolone carbon-monoxide-releasing molecule: Prodrug and albumin-assisted delivery enables anticancer and potent anti-inflammatory effects. *J. Am. Chem. Soc.* **2018**, *140*, 9721.
(38) Anderson, S. N.; Richards, J. M.; Esquer, H. J.; Benninghoff, A. D.; Arif, A. M.; Berreau, L. M. A Structurally-Tunable 3-

https://dx.doi.org/10.1021/acs.joc.9b03248
J. Org. Chem. XXXX, XXX, XXX−XXX

Hydroxyflavone Motif for Visible Light-Induced Carbon Monoxide-Releasing Molecules (CORMs). *ChemistryOpen* **2015**, *4*, 590.
(39) Berreau, L. M.; Anderson, S. N. US Patent 9,840,488 B2, 2017.
(40) Dávila, Y. A.; Sancho, M. I.; Almandoz, M. C.; Blanco, S. E. Solvent Effects on the Dissociation Constants of Hydroxyflavones in Organic−Water Mixtures. Determination of the Thermodynamic pK_a Values by UV−Visible Spectroscopy and DFT Calculations. *J. Chem. Eng. Data* **2013**, *58*, 1706.
(41) Duarte, L. G. T. A.; Germino, J. C.; de Ávila Braga, C.; Barboza, C. A.; Atvars, T. D. Z.; da Silveira Santos, F.; Rodembusch, F. S. Photoacidity as a tool to rationalize excited state intramolecular proton transfer reactivity in flavonols. *Photochem. Photobiol. Sci.* **2018**, *17*, 231.
(42) Rossini, E.; Bochevarov, A. D.; Knapp, E. W. Empirical Conversion of pKa Values between Different Solvents and Interpretation of the Parameters: Application to Water, Acetonitrile, Dimethyl Sulfoxide, and Methanol. *ACS Omega* **2018**, *3*, 1653.
(43) McMorrow, D.; Kasha, M. Intramolecular excited-state proton transfer in 3-hydroxyflavone. Hydrogen-bonding solvent perturbations. *J. Phys. Chem.* **1984**, *88*, 2235.
(44) Wolfbeis, O. S.; Knierzinger, A.; Schipfer, R. pH-dependent fluorescence spectroscopy XVII: first excited singlet state dissociation constants, phtootautomerism and dual fluorescence of flavonol. *J. Photochem.* **1983**, *21*, 67.
(45) Dereka, B.; Letrun, R.; Svechkarev, D.; Rosspeintner, A.; Vauthey, E. Excited-state dynamics of 3-hydroxyflavone anion in alcohols. *J. Phys. Chem. B* **2015**, *119*, 2434.
(46) Young, R. H.; Brewer, D.; Keller, R. A. Determination of rate constants of reaction and lifetimes of singlet oxygen in solution by a flash photolysis technique. *J. Am. Chem. Soc.* **1973**, *95*, 375.
(47) Nagai, S.; Ohara, K.; Mukai, K. Kinetic study of the quenching reaction of singlet oxygen by flavonoids in ethanol solution. *J. Phys. Chem. B* **2005**, *109*, 4234.
(48) Haag, W. R.; Gassman, E. Singlet oxygen in surface waters—Part I: Furfuryl alcohol as a trapping agent. *Chemosphere* **1984**, *13*, 631.
(49) Montalti, M.; Credi, A.; Prodi, L.; Gandolfi, M. T. *Handbook of photochemistry*; CRC Press, 2006.
(50) Itoh, M.; Fujiwara, Y. The ground state tautomer in the excited state relaxation process of 3-hydroxyflavone at room temperature. *Chem. Phys. Lett.* **1986**, *130*, 365.
(51) Al Anshori, J.; Slanina, T.; Palao, E.; Klan, P. The internal heavy-atom effect on 3-phenylselanyl and 3-phenyltellanyl BODIPY derivatives studied by transient absorption spectroscopy. *Photochem. Photobiol. Sci.* **2016**, *15*, 250.
(52) Loco, D.; Protti, S.; Mennucci, B.; Mezzetti, A. Critical assessment of solvent effects on absorption and fluorescence of 3HF in acetonitrile in the QM/PCM framework: A synergic computational and experimental study. *J. Mol. Struct.* **2019**, *1182*, 283.
(53) Chou, P.-T.; Martinez, M. L. Photooxygenation of 3-hydroxyflavone and molecular design of the radiation-hard scintillator based on the excited-state proton transfer. *Radiat. Phys. Chem.* **1993**, *41*, 373.
(54) Brewer, W. E.; Studer, S. L.; Standiford, M.; Chou, P. T. Dynamics of the triplet state and the reverse proton transfer of 3-hydroxyflavone. *J. Phys. Chem.* **1989**, *93*, 6088.
(55) Chou, P. T.; Studer, S. L.; Martinez, M. L.; Orton, E.; Young, M. Photooxygenation of 3-Hydroxyflavone in a 12 K O_2 Matrix. *Photochem. Photobiol.* **1991**, *53*, 587.
(56) Montana, P.; Pappano, N.; Debattista, N.; Avila, V.; Posadaz, A.; Bertolotti, S. G.; Garcia, N. A. The activity of 3-and 7-hydroxyflavones as scavengers of superoxide radical anion generated from photo-excited riboflavin. *Can. J. Chem.* **2003**, *81*, 909.
(57) Szakács, Z.; Kállay, M.; Kubinyi, M. Theoretical study on the photooxygenation and photorearrangement reactions of 3-hydroxyflavone. *RSC Adv.* **2017**, *7*, 32185.
(58) Yokoe, I.; Higuchi, K.; Shirataki, Y.; Komatsu, M. Photochemistry of flavonoids. III. Photorearrangement of flavonols. *Chem. Pharm. Bull.* **1981**, *29*, 894.
(59) Nani, R. R.; Gorka, A. P.; Nagaya, T.; Kobayashi, H.; Schnermann, M. J. Near-IR light-mediated cleavage of antibody−drug conjugates using cyanine photocages. *Angew. Chem., Int. Ed.* **2015**, *54*, 13635.
(60) Nani, R. R.; Gorka, A. P.; Nagaya, T.; Yamamoto, T.; Ivanic, J.; Kobayashi, H.; Schnermann, M. J. In Vivo Activation of Duocarmycin−Antibody Conjugates by Near-Infrared Light. *ACS Cent. Sci.* **2017**, *3*, 329.
(61) Mondal, R.; Shah, B. K.; Neckers, D. C. Synthesis and Photophysical Properties of Dihydroheptacenes: New Blue-Emitting Materials. *J. Org. Chem.* **2006**, *71*, 4085.
(62) He, M.; Chen, G.; Huang, X.; Xu, R.; Zeng, Z.; Yang, J. *N*-Phthaloyltranexamic acid ammonium salt derivatives as photocaged superbase for redox free radical photopolymerization. *Polym. Chem.* **2014**, *5*, 2951.
(63) Gandin, E.; Lion, Y.; Van de Vorst, A. Quantum yield of singlet oxygen production by xanthene derivatives. *Photochem. Photobiol.* **1983**, *37*, 271.
(64) Solomek, T.; Heger, D.; Ngoy, B. P.; Givens, R. S.; Klan, P. The pivotal role of oxyallyl diradicals in photo-Favorskii rearrangements: transient spectroscopic and computational studies. *J. Am. Chem. Soc.* **2013**, *135*, 15209.
(65) Tomasi, J.; Mennucci, B.; Cammi, R. Quantum mechanical continuum solvation models. *Chem. Rev.* **2005**, *105*, 2999.
(66) Stephens, P. J.; Devlin, F.; Chabalowski, C.; Frisch, M. J. Ab initio calculation of vibrational absorption and circular dichroism spectra using density functional force fields. *J. Phys. Chem.* **1994**, *98*, 11623.
(67) Becke, A. D. Density-functional thermochemistry. III. The role of exact exchange. *J. Chem. Phys.* **1993**, *98*, 5648.
(68) Adamo, C.; Jacquemin, D. The calculations of excited-state properties with time-dependent density functional theory. *Chem. Soc. Rev.* **2013**, *42*, 845.
(69) Laurent, A. D.; Adamo, C.; Jacquemin, D. Dye chemistry with time-dependent density functional theory. *Phys. Chem. Chem. Phys.* **2014**, *16*, 14334.
(70) Schäfer, A.; Horn, H.; Ahlrichs, R. Fully optimized contracted Gaussian basis sets for atoms Li to Kr. *J. Chem. Phys.* **1992**, *97*, 2571.
(71) Schäfer, A.; Huber, C.; Ahlrichs, R. Fully optimized contracted Gaussian basis sets of triple zeta valence quality for atoms Li to Kr. *J. Chem. Phys.* **1994**, *100*, 5829.
(72) Frisch, M. J.; Trucks, G. W.; Schlegel, H. B.; Scuseria, G. E.; Robb, M. A.; Cheeseman, J. R.; Scalmani, G.; Barone, V.; Petersson, G. A.; Nakatsuji, H.; Li, X.; Caricato, M.; Marenich, A. V.; Bloino, J.; Janesko, B. G.; Gomperts, R.; Mennucci, B.; Hratchian, H. P.; Ortiz, J. V.; Izmaylov, A. F.; Sonnenberg, J. L.; Williams; Ding, F.; Lipparini, F.; Egidi, F.; Goings, J.; Peng, B.; Petrone, A.; Henderson, T.; Ranasinghe, D.; Zakrzewski, V. G.; Gao, J.; Rega, N.; Zheng, G.; Liang, W.; Hada, M.; Ehara, M.; Toyota, K.; Fukuda, R.; Hasegawa, J.; Ishida, M.; Nakajima, T.; Honda, Y.; Kitao, O.; Nakai, H.; Vreven, T.; Throssell, K.; Montgomery, J. A., Jr.; Peralta, J. E.; Ogliaro, F.; Bearpark, M. J.; Heyd, J. J.; Brothers, E. N.; Kudin, K. N.; Staroverov, V. N.; Keith, T. A.; Kobayashi, R.; Normand, J.; Raghavachari, K.; Rendell, A. P.; Burant, J. C.; Iyengar, S. S.; Tomasi, J.; Cossi, M.; Millam, J. M.; Klene, M.; Adamo, C.; Cammi, R.; Ochterski, J. W.; Martin, R. L.; Morokuma, K.; Farkas, O.; Foresman, J. B.; Fox, D. J. *Gaussian 16*, Rev. C.01; Gaussian, Inc.: Wallingford, CT, 2016.

https://dx.doi.org/10.1021/acs.joc.9b03248
J. Org. Chem. XXXX, XXX, XXX−XXX